

# A solution to the range-Doppler dilemma of weather radar measurements by using the SMPRF codes, practical results and a comparison with operational measurements

J. Pirttilä<sup>1</sup>, M. Lehtinen<sup>1</sup>, A. Huuskonen<sup>2</sup>, and M. Markkanen<sup>1</sup>

<sup>1</sup>Sodankylä Geophysical Observatory, Tähteläntie 112, FI-99600 Sodankylä, Finland

<sup>2</sup>Finnish Meteorological Institute, Sahaajankatu 20 E, FI-00880, Helsinki, Finland

**Abstract.** Based on the measurement principles used on Incoherent Scatter Radars, the authors have developed the SMPRF pulse code which completely solves the range-Doppler dilemma and which can be used with modern magnetron radars. Results from nearly simultaneous SMPRF and traditional fixed PRF weather radar measurements are compared.

The SMPRF-code provides enough information to produce a high-resolution measured spectrum for each range gate. The shape of these measured spectra are seldom purely Gaussian. It is possible, that more advanced raw products than just reflectivity, velocity and width can be produced with the help of these high-resolution spectra.

## 1 Introduction

The weather radar measurements, as used in the operational weather radar networks throughout the world, employ uniform transmission of pulses. When measuring radar reflectivity, a low enough pulse repetition frequency (PRF) (300 to 500 Hz) is used so that a transmitted pulse will leave the measurement volume before the next pulse is transmitted providing an unambiguous reflectivity measurements result. The maximum measurement range  $r_{max}$  is calculated as

$$r_{max} = cT/2, \quad (1)$$

where  $c$  is the velocity of the radio waves and  $T$  is the time separation between the adjacent pulses, i.e. the inverse of the PRF.

When measuring wind speed, the time separation between adjacent pulses determines the maximum velocity  $v_{max}$  that can be unambiguously measured:

$$v_{max} = \text{PRF } \lambda/4, \quad (2)$$

where  $\lambda$  is the wavelength.

These two equations show that as the PRF increases, the maximum velocity increases but the maximum unambiguous range decreases and vice versa. In the literature, this phenomenon is referred to as the range-Doppler dilemma (e.g. Doviak and Zrnic, 1993). There have been various attempts to overcome this problem (Laird, 1981; Zrnić, 1985; Gray et al., 1989; and Sachidananda and Zrnić, 1999), but these papers have only been able to provide partial solutions.

Within other fields of radio science, radar methods have been developed which are not limited by the range-Doppler dilemma. Such methods have been presented e.g. by Farley (1972), Greenwald et al. (1985) and Lehtinen and Häggström (1987) for the ionospheric radar studies. However, these solutions are not directly applicable to the weather radar case, because the continuity of the measurement is not important in the ionospheric case. Based on the principles used with the ionospheric radars the authors have developed a code for the weather radar case, called SMPRF, which stands for Simultaneous Multiple Pulse Repetition Frequency code (Lehtinen, 1999).

## 2 Theory

### 2.1 Equations

A full radar measurement model, explaining the characteristics of the measured signal correlation products to the properties of a continuous and random scattering medium is presented in Lehtinen and Huuskonen (1996) for scattering from ionized plasma in the ionospheric layers. There the concept of ambiguity functions is used to describe the way different ranges and different scattering times contribute to the estimates of the signal products when using complicated radar waveforms. In this article we suppose very short radar pulses and the formalism becomes simpler: we base the formalism on the following physically intuitive arguments:

We suppose we transmit pulses at time instances  $t_i \Delta t$  and sample them at time instances  $t \Delta t$ , where  $\Delta t$  is the sampling time interval. We suppose here that the  $t_i$  coefficients can be supposed to be integers. We also suppose, that the typical pulse length is approximately equal to  $\Delta t$ , though the following discussions do not actually need this assumption to be true.

A typical magnetron radar sends short pulses with random phases. We suppose, however, that apart from the constant phase difference the shapes of the pulses are otherwise the same. Let us choose one pulse as a reference - then the phase of each of the pulses can be described by a complex number of unit magnitude  $c_i$ . We also suppose, that the different scattering ranges are labelled by the total travel time of the pulse from transmitter to the scattering point and back to the radar again. Let us denote the response from a scattering distance  $r$ , received at time  $t$  be modelled by a coefficient  $\sigma(r, t)$ . This means that if a normalized pulse would be sent at time  $t - r$ , the signal sampled at time  $t$  would be given by  $\sigma(r, t)$ . However, instead of sending a normalized pulse at time  $t - r$ , we send a series of pulses at times  $t_i$  at random phases  $c_i$  and the sampled signal at time  $t$  is thus the sum

$$z(t) = \sum_i c_i \sigma(t - t_i, t) \quad (3)$$

While the signals  $\sigma(r, t)$  depend on scattering at range  $r$ , the information carried by them is not easy to interpret directly. Typically, this signal is a sum of signals from a great quantity of elementary scatters from mutually independent scattering volumes inside the region defined by the time instant  $t$  and the duration of the elementary pulse supposed to be sent at  $t - r$ . Because of being a sum of independent and (practically) equally distributed contributions, it is a zero-mean Gaussian variable, which can obtain any (random) value allowed by its variance.

The expectation of its square is proportional to the scattering power at range  $r$ , and because of this, the crossed products of the signal are customarily used in data analysis rather than the signal itself. The expectations of the signal products are given by

$$\langle z(t) \overline{z(t')} \rangle = \sum_i c_i \overline{c_j} \langle \sigma(t - t_i, t) \overline{\sigma(t' - t_j, t')} \rangle \quad (4)$$

The key point to note is that the scattering from different ranges cannot correlate with each other. The reason for this is that the phase of  $\sigma(t - t_i, t)$  is a random quantity, depending on the constructive/destructive interference of the scatters from all the different droplets in the scattering volume. The different scattering volumes in the sum are typically at least tens of kilometers apart from each other and there cannot be any kind of coherence between these volumes in the scale defined by the radar wavelength. Thus,

$$\langle \sigma(t - t_i, t) \overline{\sigma(t' - t_j, t')} \rangle = 0, \text{ if } t - t_i \neq t' - t_j, \quad (5)$$

which leads to the following equation for the signal power ( $t = t'$ ):

$$\langle z(t) \overline{z(t)} \rangle = \sum_i \sum_j c_i \overline{c_j} \langle \sigma(t - t_i, t) \overline{\sigma(t - t_j, t)} \rangle$$

$$= \sum_i |c_i|^2 |\sigma(t - t_i, t)|^2 \quad (6)$$

If the separations of the transmitted pulses at times  $t_i$  are shorter than the range extent of the target, several pulses contribute simultaneously to the signal power and this formula can be used to model the relationship of the signal power  $|z(t)|^2$  to the range-dependent scattering power  $|\sigma(t - t_i, t)|^2$ .

## 2.2 Scattering lag estimates

Doppler measurements depend on lagged product estimates, where the signal sample corresponding to a certain range is correlated with another signal sample corresponding to the same range but measured at a differing time. Equation (4) can be used to describe the relationships of different lagged products to the range and lag values they correspond to.

Contributions to the sum (4) can only come from those cases where the two ranges are the same:

$$t - t_i = t' - t_j \Leftrightarrow t - t' = t_i - t_j \quad (7)$$

Thus, only those lag values can be estimated, which correspond to a separation of transmission times of two different pulses in the transmission.

If the pulse separations are chosen properly, it is possible to choose their timing so that in lag estimation only one height contributes in the sum (4).

## 3 Practical results

### 3.1 Measurement setup

The Finnish Meteorological Institute operates a weather radar on top of the Luosto fell (67°08' N, 26°54' E, 514 above MSL). The Luosto radar is a C-band weather radar with a 250 kW magnetron transmitter built by Gematronik. In the operational use, the transmitter is controlled by the Sigmet RVP7 signal processor, and the signal is processed and analyzed by Sigmet's IRIS software.

The Luosto radar was used for the development of the SMPRF code. During these measurements IRIS was used to control only the antenna, while rest of the radar was operated using custom electronics and software. During the measurements discussed in this paper, only the IQ time series were stored to a hard disk. The rest of the signal processing and data analysis was performed afterwards off-line.

The measurements were arranged so that immediately after the SMPRF measurement an IRIS measurement was carried out. The actual time difference was 2 min. In the following, the results based on the Sigmet IRIS system will be called as FMI or operational results and the results from the custom measurement the SMPRF results.

The data for this study was collected at the Luosto radar in the morning of 21 August 2003. The measured weather consisted of a front with some precipitation extending in the southwest-east direction about 220–290 km from the radar. The wind was not very spectacular, the maximum speed was

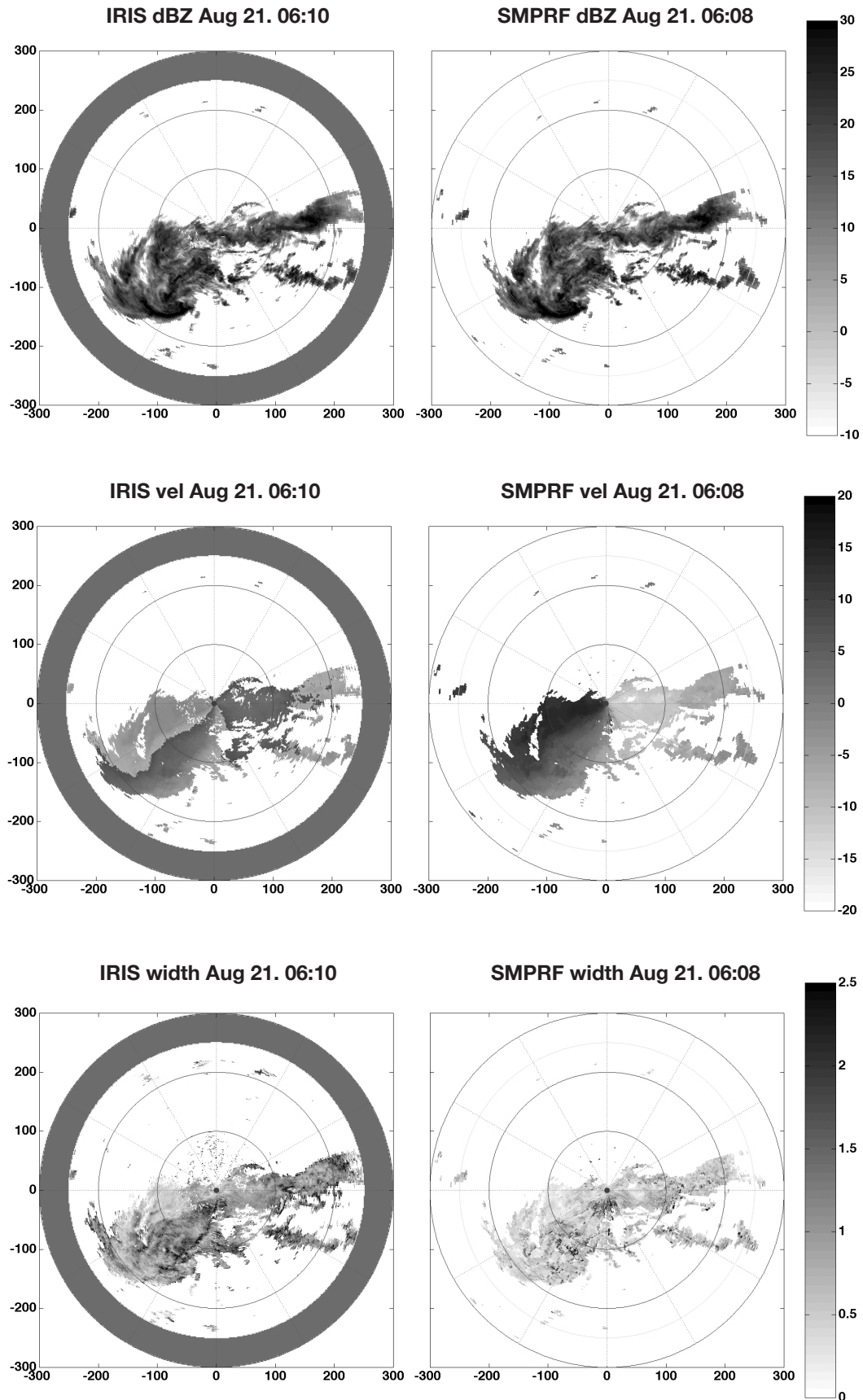


**Fig. 1.** Results from the operational scan (left column) and the SMPRF scan (right column).

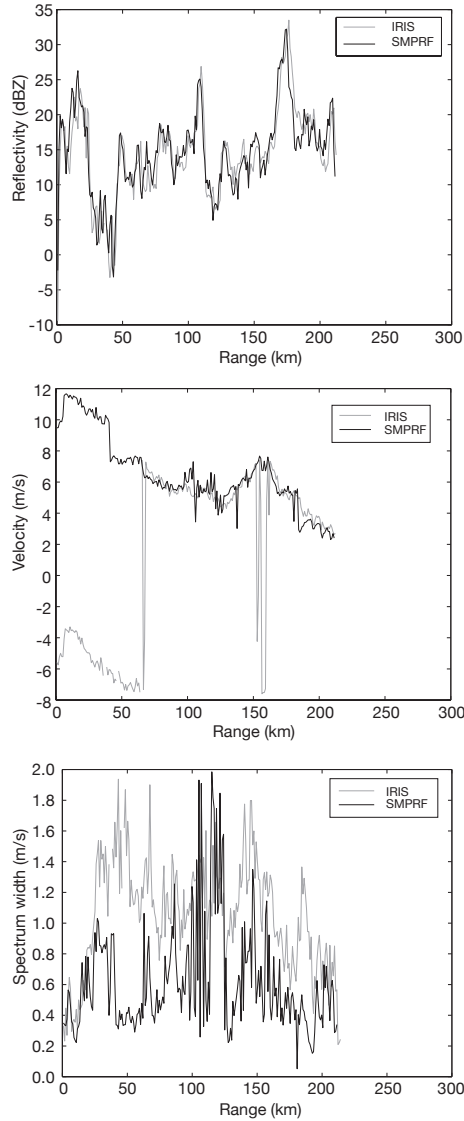


**Fig. 2.** Parameter profiles from IRIS and SMPRF at azimuth  $225^\circ$ .

$17.5 \text{ ms}^{-1}$ , still high enough to cause problems for the operational measurement.

During this event the SMPRF solution was based on  $2 \mu\text{s}$  pulses with an effective PRF of 480 Hz. The maximum range for the SMPRF measurement was 300 km and the velocity span was  $-53 \text{ ms}^{-1} \dots 53 \text{ ms}^{-1}$ . In the SMPRF method both the maximum range and the maximum velocity can be freely chosen, but in practise we are constrained by the limitations posed by the transmitter and the receiver performances. The operational FMI scan was a standard pulse train of  $2 \mu\text{s}$  pulses (PRF 570 Hz) having the maximum range of 250 km and the folding velocity of  $7.5 \text{ ms}^{-1}$ . In both cases the antenna rotated with a speed of  $10^\circ/\text{s}$  and the elevation angle was  $0.1^\circ$ . The angular resolution was the standard  $1^\circ$ , and thus each ray was measured in 0.1 s.

### 3.2 Reflectivity results

Figure 1 shows the results from both the operational and the SMPRF scan. All the figures have the same scale: the maximum range is 300 km. Because of the difference in maximum ranges of the measurements, the operational results are shaded with gray beyond 250 km range. Also, we have drawn a light gray circle on the SMPRF images to help to distinguish what is unseen at the far ranges in the operational scan. The dark grey circles denote the 100 km range intervals.

The top row of the Fig. 1 shows the radar reflectivity results. The precipitation area is oriented mostly in an east-west direction extending about 270 km to the east and 220 km to the southwest. In the north-south direction the dimension of the precipitation area is about 100 km. The reflectivity fields are strikingly similar despite of the two minute time difference between the scans. Top panel of Fig. 2 compares reflectivity profiles from both scans at the azimuth of  $225^\circ$ . One can clearly see that both curves “walk hand in hand” and the differences are most probably due to the time difference between the scans.

### 3.3 Velocity results

Middle row of Fig. 1 shows velocity results from both scans. The velocity results are evidently folded and ambiguous. The velocity results of the SMPRF scan are between  $-16.4 \text{ ms}^{-1} \dots 17.5 \text{ ms}^{-1}$ , and no folding has appeared.

Middle panel of Fig. 2 compares velocity profiles from both scans at the azimuth  $225^\circ$ . Velocity profile from the SMPRF code shows unambiguous velocities between  $1.7 \text{ ms}^{-1} \dots 11.7 \text{ ms}^{-1}$ , whereas the velocity profile from the operational scan is partly folded.

The velocity profile from the SMPRF code shows a steep step at 50 km range. Similar steps or small spikes can be seen in the velocity profile at ranges beyond 100 km. The reason for these steps and spikes can be understood by examining the ACF data produced by the SMPRF code. Right panel of Fig. 3 shows the power spectrum of the measured signal. The spectrum clearly reveals, that the scattering volume contains four wind velocity peaks.

Our fitting procedure fits a Gaussian ACF around the velocity that has the most power within the scattering volume. If there are two almost equally strong wind velocity peaks, the fitted velocity can jump sharply from gate to gate as fitting procedure chooses the stronger of the two at each gate. This explains the steps and small spikes seen in the velocity profile.

### 3.4 Spectral width

Bottom row of Fig. 1 shows spectrum width results from both scans. The width results of the operational scan are less than  $4.7 \text{ ms}^{-1}$ . The width results of the SMPRF scan are less than  $3.7 \text{ ms}^{-1}$  and in many places smaller than the width estimates from the operational scan. However, the results are closely

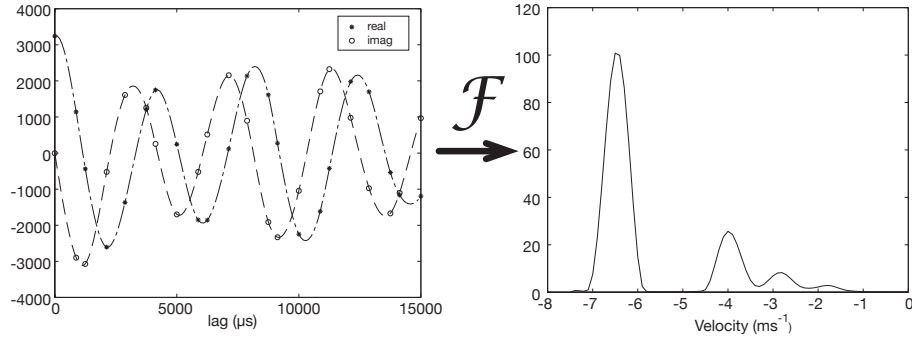


**Fig. 3.** Measured autocorrelation samples and the corresponding spectrum.

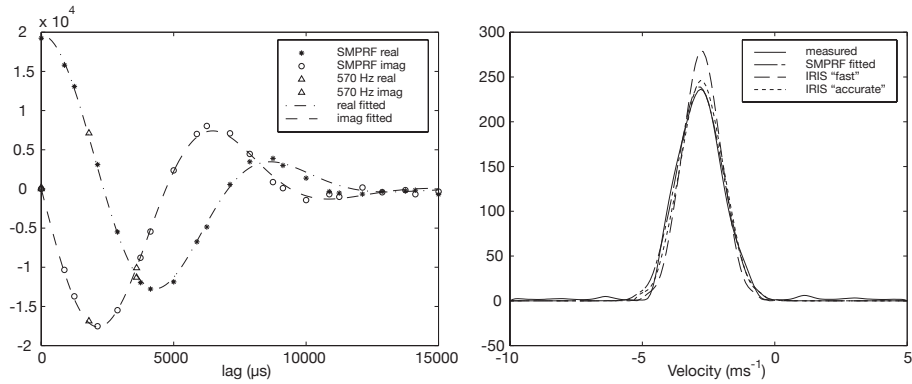


**Fig. 4.** Measured autocorrelation samples that fit well to the Gaussian spectrum model, the corresponding spectrum and spectra of different analysis results.

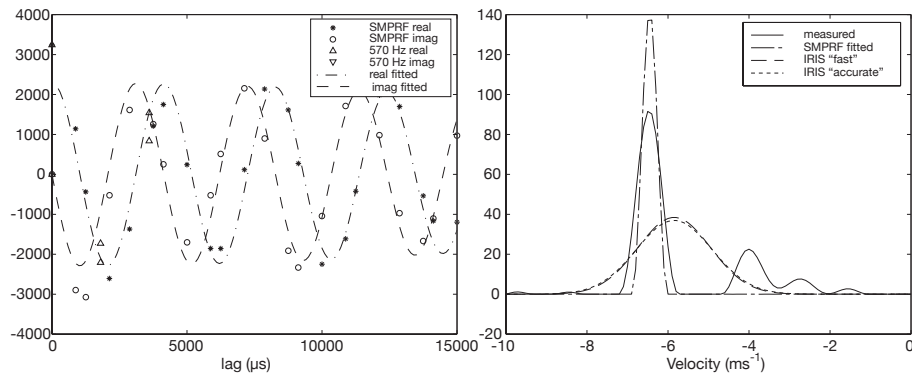


**Fig. 5.** Measured autocorrelation samples that do not fit to the Gaussian spectrum model, the corresponding spectrum and spectra of different analysis results

identical at places. For example there is a continuous area of larger widths just south of the radar at 10 km...40 km ranges.

Bottom panel of Fig. 2 compares width profiles from both scans at the azimuth of 225°. Between ranges from 25 km to 90 km the SMPRF widths are significantly smaller than the widths from the operational scan.

As the full spectrum from the operational scan is not available, any explanation for this and other differences in the width estimates can only be given by examining the ACF data produced by the SMPRF code and by calculating spectral estimates with various methods.

For this purpose we can use the almost Gaussian ACF shown in the left panel of Fig. 3 and the clearly non-Gaussian case shown in the right panel of Fig. 3. Spectrum parameters are analyzed from both ACFs using the two methods: the fitting and the direct parameter estimation.

The direct parameter estimation methods used by IRIS are applicable only when the autocorrelation samples are calculated from an evenly spaced pulse train. To enable the use of these simple direct methods, the autocorrelation samples at lags 0, 1800 and 3600  $\mu\text{s}$  were interpolated from the original SMPRF-generated samples by spline interpolation. These values are denoted by triangles in the autocorrelation panels of the Figs. 4 and 5.

The real shape of the spectrum was calculated directly from the autocorrelation samples using the statistical inversion analysis. Also, to get the SMPRF-estimate of the spectrum parameters, a Gaussian autocorrelation function was fitted to the autocorrelation samples using the Levenberg-Marquardt algorithm. The fitted ACF is denoted in the left panels of Figs. 4 and 5 by dashed line. Lastly, two IRIS-estimates of the spectrum parameters were calculated from the three interpolated lags using the direct methods presented in the IRIS User's Manual. From these parameters three Gaussian spectra was calculated: SMPRF fitted, IRIS "accurate" and IRIS "fast", which were plotted together with the measured spectrum in the right panels of Figs. 4 and 5.

Figure 4 shows that when the measured autocorrelation samples fit well to the Gaussian spectrum model and the noise is small compared to the values of the autocorrelation estimates all the methods to estimate the width of the spectrum produce very similar results.

As soon as the autocorrelation samples deviate slightly from the Gaussian spectrum model, the direct methods to obtain the width estimate start to produce wrong results.

In the non-Gaussian case the Levenberg-Marquardt fitting used in the SMPRF analysis finds the strongest velocity peak of the spectrum. The velocity estimate is then the velocity where most of the power is. The width estimate becomes narrower than the width of the highest velocity peak.

## 4 Conclusions

The results of this paper show that the Simultaneous Multiple Pulse Repetition Code is able to solve the long standing problem of the weather radar measurements, the range-Doppler dilemma. This method allow us to choose freely both the maximum range to be measured and the maximum velocity to be determined, and there is no restriction posed to the first based on the choice of other one.

The SMPRF code produces a large number of autocorrelation samples, which can be used to estimate the spectrum parameters. The present way to analyze the spectrum width is based on the assumption of a Gaussian spectrum shape. However, as is also clearly seen in the spectra shown in this paper, they often look like a sum of two or more Gaussian spectra or may even have a form more complicated than that.

Physically, the spectrum shape is closely related to the velocity distribution of the target scattering droplets. It is plausible to suppose that this is a distribution, which is peaked around the average wind velocity and has a shape around that with the spread caused by the atmospheric turbulence.

More robust estimates of the spectrum parameters can be produced, if the Gaussian spectral theory can be replaced with more advanced model, that allows more freedom in the shape of the spectrum. It is also possible, that more advanced raw products than just reflectivity, velocity and width can be produced with the help of more advanced spectrum model.

*Acknowledgements.* The Finnish Meteorological Institute is gratefully acknowledged for providing the IRIS data used in this work. Financial support from Technology Development Centre Finland (Tekes) is gratefully acknowledged.

## References

- Doviak, R. J. and Zrnic, D. S.: Doppler radar and weather observations. Academic Press Inc, San Diego, CA, 562 pp., 1993.
- Evans, S. N. and Stark, P. B.: Inverse problems as statistics, *Inverse Problems*, No 18, pp 55–97, 2002.
- Farley, D. T.: Multiple-pulse incoherent-scatter correlation function measurements, *Radio Sci.*, 7, 661–666, 1972.
- Gray, G., Lewis B., Vinson J., and Pratte, F.: A real time implementation of staggered PRT velocity unfolding, *J. Atmos. Oceanic Tech.*, 6, pp. 186–187, 1989.
- Greenwald, R. A., Baker, K. B., Hutchins, R. A., and Hanuise, C.: An HF phased-array radar for studying small-scale structure in the high-latitude ionosphere, *Radio Sci.*, 20, 63–79, 1985.
- Lehtinen, M. S.: U.S. Patent No. 6,232,913., Method and system for measuring radar reflectivity and Doppler shift by means of a pulse radar, 1999.
- Lehtinen, M. S. and Huuskonen, A.: General incoherent scatter analysis and GUISDAP, *J. Atmos. Terr. Phys.*, 58, 435–452, 1996.
- Lehtinen, M. S. and Häggström, I.: A new modulation principle for incoherent scatter measurements, *Radio Sci.*, 22, 625–634, 1987.
- Sachidananda, M. and Zrnić, D. S.: Systematic Phase Codes for Resolving Range Overlaid Signals in a Doppler Weather Radar., *J. Atmos. Oceanic Technol.*, 16, pp. 1351–1363, 1999.
- Laird, B. G.: On ambiguity resolution by random phase processing, 20th Conf. Radar Met., AMS, pp. 327–331, 1981.
- Sigmat Inc.: RVP 7 User's Manual, <ftp://ftp.sigmet.com/outgoing/manuals/rvp7user>, 2000.
- Zrnić, D. S., and Mahapatra P.: Two methods of ambiguity resolution in pulse Doppler weather radars, *IEEE Trans. Aerosp. Electron. Syst.*, AES-21, pp. 470–483, 1985.